Electronic Supplementary Material (ESI) for Physical Chemistry Chemical Physics.

Supporting Information

P-Incorporated CuO/Cu_2S Heteronanorods as an Efficient Electrocatalyst for Glucose Oxidation Reaction toward Highly Sensitive and Selective Glucose Sensing

L. L. D. Thi[1,2,*], Thi H. Ho[3,4], Tuan V. Vu[3,4], Dang L. T. Nguyen[1,2], Minh Xuan Tran[1,2],
Sonny H. Rhim[5], C-D. Nguyen[6,#]

[1]Laboratory for Advanced Nanomaterials and Sustainable Energy Technologies, Institute for Computational Science and Artificial Intelligence, Van Lang University, Ho Chi Minh City, Vietnam.

[2]Faculty of Applied Technology, School of Technology, Van Lang University, Ho Chi Minh City, Vietnam.

[3]Laboratory for Computational Physics, Institute for Computational Science and Artificial Intelligence, Van Lang University, Ho Chi Minh City, Vietnam

[4]Faculty of Mechanical - Electrical and Computer Engineering, School of Technology, Van Lang University, Ho Chi Minh City, Vietnam.

[5]Department of Physics and Energy Harvest Storage Research Center, University of Ulsan, Ulsan, 44610, Republic of Korea

[6]The University of Danang - University of Science and Education, Danang 550000, Vietnam.

[*,#]Corresponding author.

[*]Corresponding author at: Laboratory for Advanced Nanomaterials and Sustainable Energy Technologies, Institute for Computational Science and Artificial Intelligence, Van Lang University, Ho Chi Minh City, Vietnam.

E-mail address: luyen.doanthiluu@vlu.edu.vn (Dr. L. L. D. Thi) cdn@ued.udn.vn (Dr.C-D. Nguyen)

Experimental

Preparation of CuO NRs

The $Cu(OH)_2$ NRs sample was initially synthesized by chemical oxidation method. Next, the obtained $Cu(OH)_2$ NRs were calcinated at 300 °C for 2 h to convert into the CuO NRs sample.

Preparation of CuO/Cu_2S h-NRs

The as-synthesized $Cu(OH)_2$ NRs sample was immersed in 0.1 M thiourea solution at 90 °C for 5 h to partially convert into Cu_2S, followed by annealing at 300 °C for 2 h to form CuO/Cu_2S h-NRs sample.

Density function theory (DFT) calculations

We performed DFT calculations using the Vienna ab initio simulation package (VASP) [1,2]. The projector-augmented wave (PAW) method was employed to describe the interactions between the core and valance electrons [3]. The exchange-correlation potential was treated by the generalized gradient approximation (GGA) parameterized by the Perdew-Burke-Ernzerhof (PBE) functional [4]. The DFT-D3 correction within the Grimme scheme was applied for the long-range van der Waals interactions between atoms [5]. An energy cutoff of 400 eV was chosen for wave function expansion. For Brillouin zone-sampling, all calculations were performed at the Γ-point. The energy and force convergences were set at 10^{-6} eV and 10^{-2} eV/Å, respectively. The adsorption energy of glucose was calculated as the following equation:

$$E_{ads} = E_{Glu + CuO/Cu_2S} - E_{Glu} - E_{CuO/Cu_2S} \tag{1}$$

where $E_{Glu + CuO/Cu_2S}$, is the total energy of glucose-adsorbed CuO/Cu_2S system; E_{Glu}, E_{CuO/Cu_2S} are the total energies of isolated glucose and CuO/Cu_2S, respectively. In addition, differential charge density and Bader charge analysis were performed to investigate the charge transfer between glucose and CuO/Cu_2S [6].

According to experimental results, the CuO and Cu_2S were preferentially growing along the (111) and (220) planes. Hence, the CuO/Cu_2S system was simulated by a squared unit cell with a lattice constant of 15 Å, and CuO(111) and Cu_2S(220) were horizontally connected, as shown in Figure 8. Then, the P-CuO/Cu_2S system was constructed by substituting P into O and S atoms. For structural optimization, the CuO/Cu_2S and P-CuO/Cu_2S systems were allowed to be fully relaxed. After all, the glucose molecule was put and relaxed on those surfaces. A vacuum spacing of 20 Å was chosen to avoid image interactions between neighboring slabs.

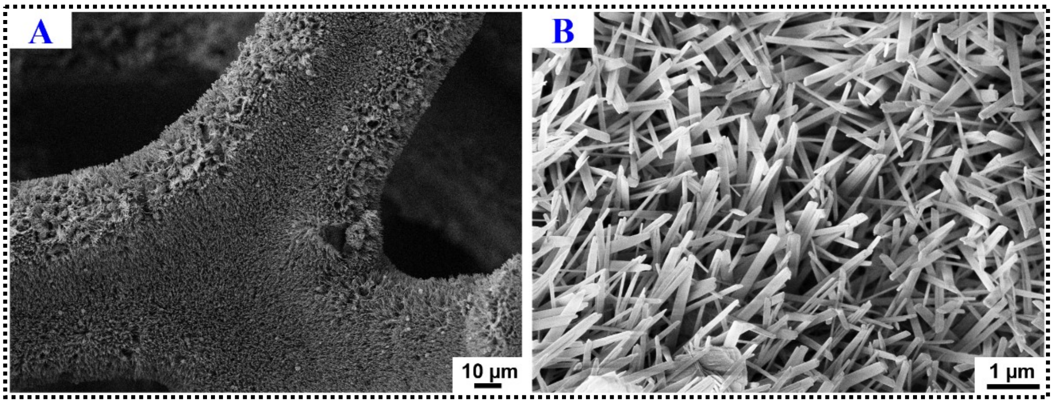

Figure S1. SEM images at different magnifications of $Cu(OH)_2$ NRs.

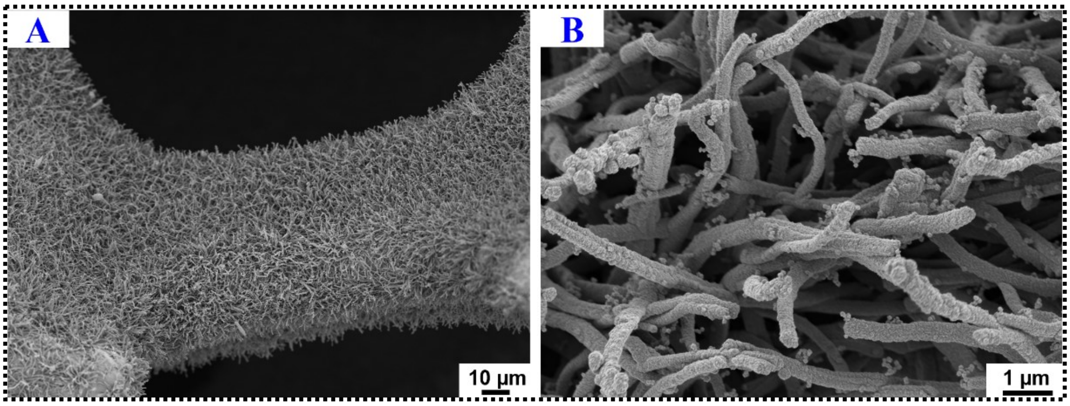

Figure S2. SEM images at different magnifications of CuO/Cu_2S h-NRs.

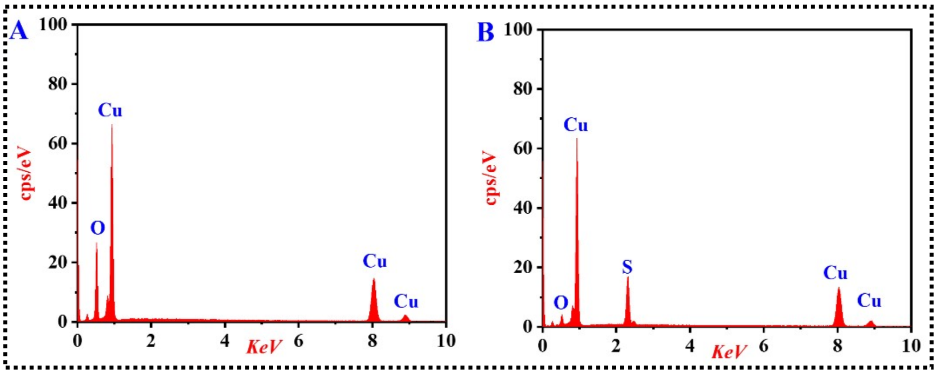

Figure S3. EDS patterns of (a) $Cu(OH)_2$ NRs and (b) CuO/Cu_2S h-NRs.

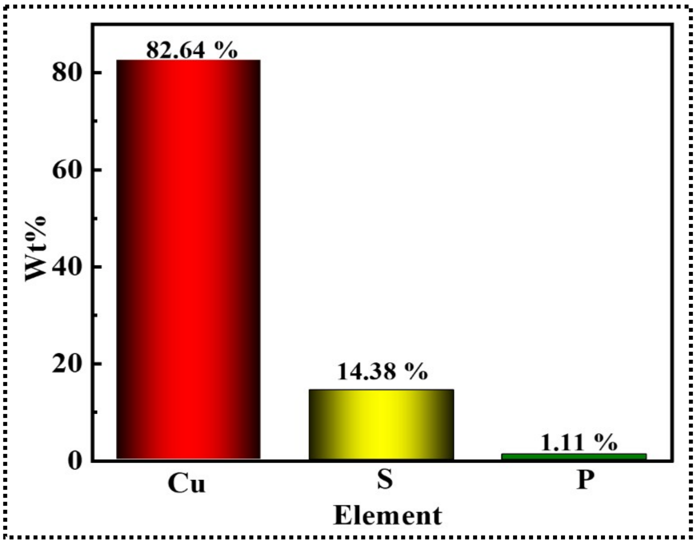

Figure S4. Weight percentages of Cu, S, and P elements in the P-CuO/Cu_2S h-NRs from the ICP-OES measurement.

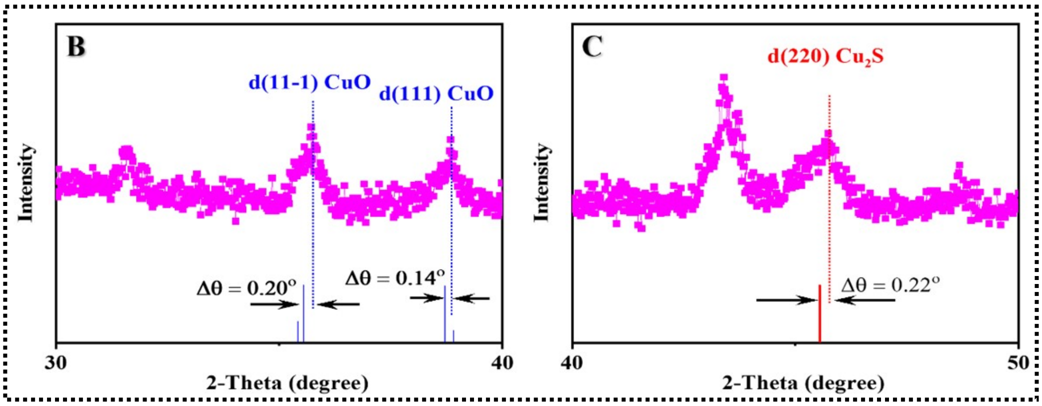

Figure S5. Magnified view of XRD pattern from the proposed P-CuO/Cu_2S h-NRs and standard samples: (a) pure CuO and (b) pure Cu_2S.

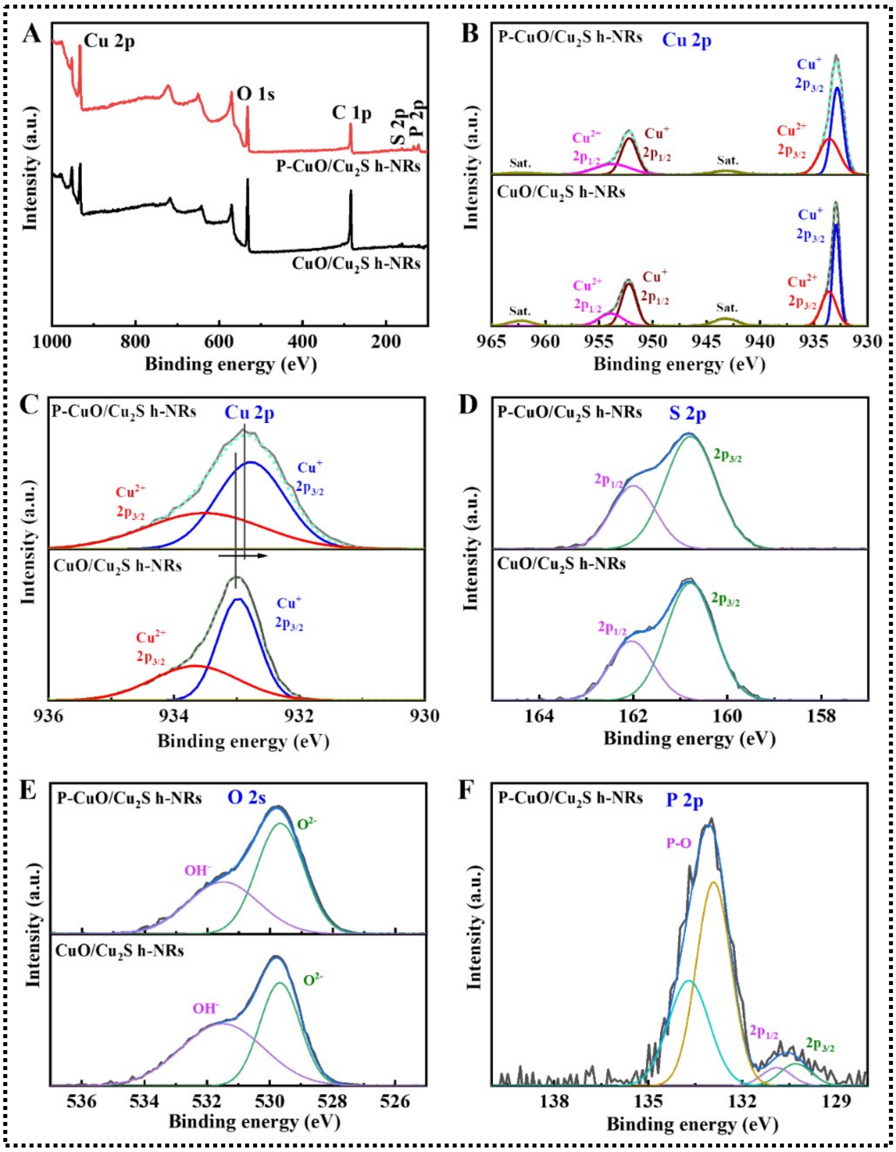

Figure S6. (a) XPS survey spectra of the P-CuO/Cu$_2$S h-NRs and CuO/Cu$_2$S h-NRs. High-resolution XPS spectra of (b) Cu 2p, (c) S 2p, and (d) O 1s in the P-CuO/Cu$_2$S h-NRs and CuO/Cu$_2$S h-NRs.

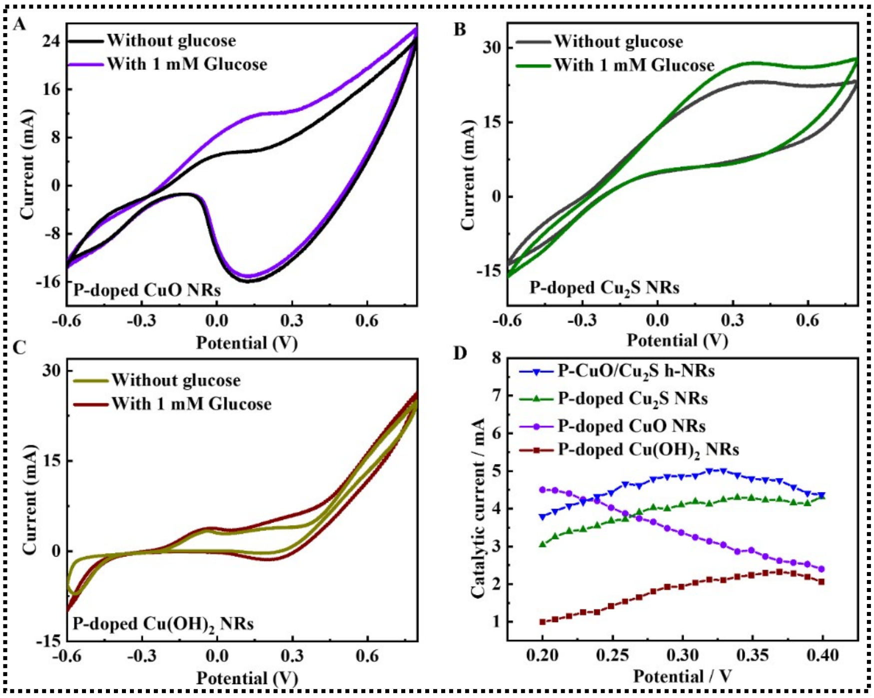

Figure S7. CV curves of (a) P-doped CuO NRs, (b) P-doped Cu_2S NRs, and (c) P-doped $Cu(OH)_2$ NRs without and with glucose. (e) The corresponding catalytic current responses of the products at different potentials.

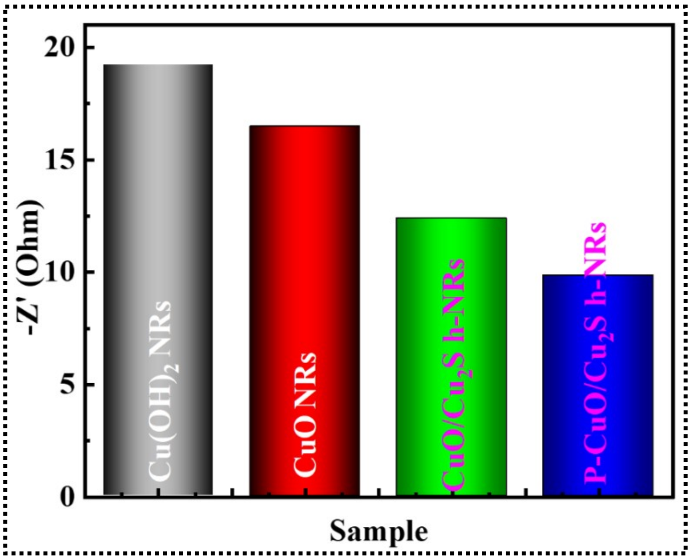

Figure S8. The corresponding charge transfer resistance values of the products: $Cu(OH)_2$ NRs, CuO NRs, CuO/Cu_2S h-NRs, and P-CuO/Cu_2S h-NRs.

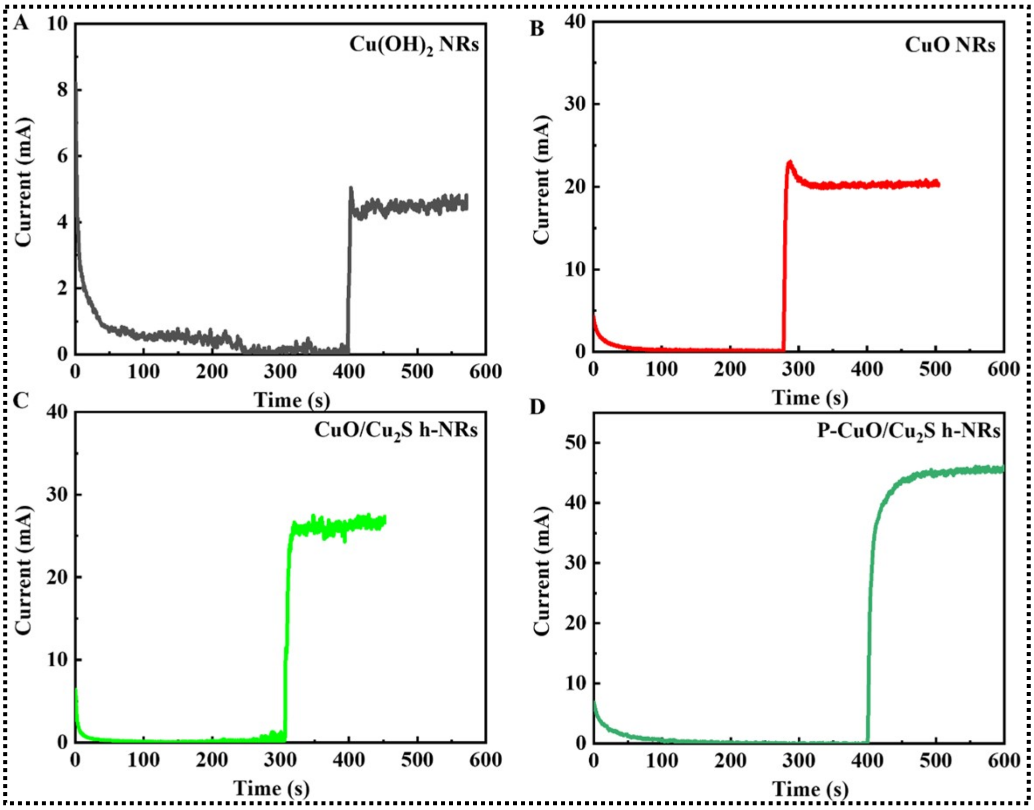

Figure S9. Chronoamperometric curves of (a) Cu(OH)$_2$ NRs, (b) CuO NRs, (c) CuO/Cu$_2$S h-NRs, and (d) P-CuO/Cu$_2$S h-NRs with glucose.

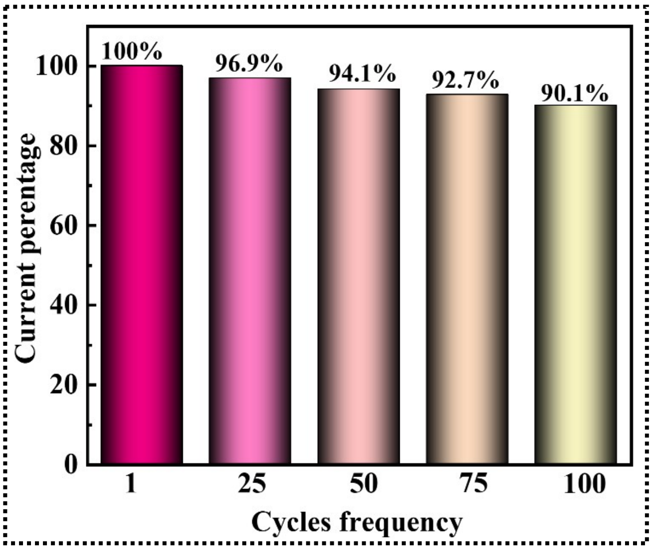

Figure S10. Peak catalytic currents of the P-CuO/Cu_2S h-NRs versus cycle frequencies (1, 25, 50, 75, and 100 cycles).

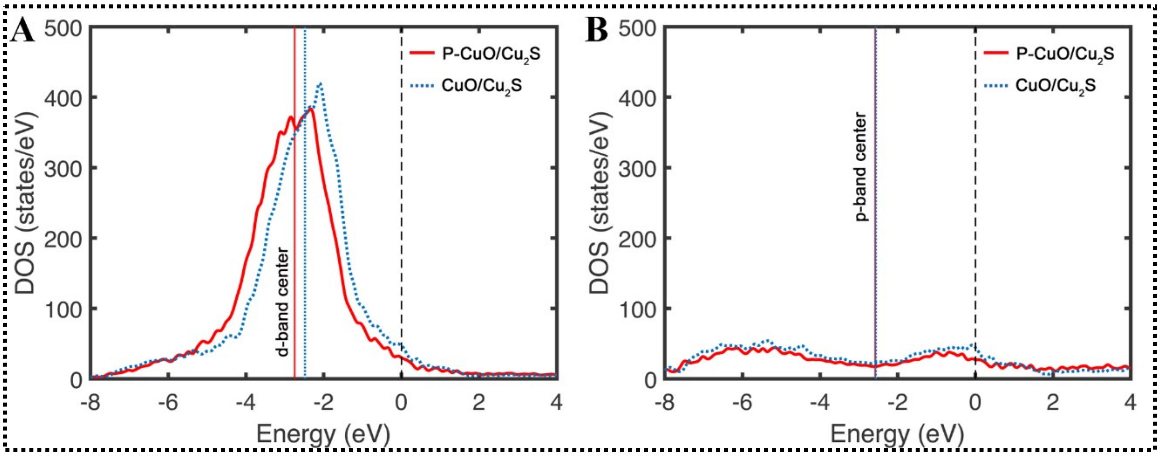

Figure S11. Partial DOS of CuO/Cu$_2$S and P-CuO/Cu$_2$S for (a) d-band center and (b) p-band center analysis. Red solid and blue dotted lines denote P-CuO/Cu$_2$S and CuO/Cu$_2$S, respectively. The Fermi level (E_F) is set to zero.

Table S1. Comparison of sensitivity and LOD values from different electrocatalysts for glucose oxidation.

Electrode materials	LOD (μM)	Linear range (mM)	Reference
MIP meicelles	0.36	1.8–36	Adv Mat Res, Trans Tech Publ., 1052 (2014), 215-219
RGO-PAMAM-Ag-GOD-CS/GCE	0.81	5.76–340.2	Biosens. Bioelectron., 36 (2012), 179-185
Au NPs/NiOH NNs	0.12	5.76–340.2	Biosens. Bioelectron., 36 (2012), 179-185
CA	0.71	0.72–2430	Mater. Chem. Phys., 187 (2017), 28-38
MIP (SPCE)	0.03	0.06–180	Biosens. Bioelectron., 91 (2017), 276-283
MIP	0.59	0.5–50	Mater. Sci. Eng. C 98, (2019) 1196-1209
P-CuO/Cu_2S h-NRs	0.95	0.02-8.2	Present work

Table S2. Adsorption energy of glucose on different positions of CuO/Cu_2S and P-CuO/Cu_2S surfaces. The more negative value indicates the more favorable adsorption.

Structure	Adsorption site	Adsorption energy (eV)
CuO/Cu_2S	Interface	-1.173
	CuO	-0.063
	Cu_2S	0.058
P-CuO/Cu_2S	Interface	-1.470
	CuO	-0.744
	Cu_2S	-0.309

Table S3. Bader charge transfer of each element to the glucose molecule in CuO/Cu_2S and P-CuO/Cu_2S. The positive and negative values indicate the charge accumulation and depletion, respectively. The rightmost value is the sum of charge transfer.

Structure	Element	Charge transfer (e^-)	
CuO/Cu_2S	Cu	-0.559	-0.763
	O	0.017	
	S	-0.222	
P-CuO/Cu_2S	Cu	-0.524	-0.766
	O	-0.003	
	S	-0.059	
	P	-0.180	

Reference

1 G. Kresse and J. Furthmüller, Efficient iterative schemes for ab initio total-energy calculations using a plane-wave basis set, *Phys. Rev. B*, 1996, **54**, 11169–11186.

2 G. Kresse and J. Furthmüller, Efficiency of ab-initio total energy calculations for metals and semiconductors using a plane-wave basis set, *Comput. Mater. Sci.*, 1996, **6**, 15–50.

3 G. Kresse and D. Joubert, From ultrasoft pseudopotentials to the projector augmented-wave method, *Phys. Rev. B*, 1999, **59**, 1758–1775.

4 J. P. Perdew, K. Burke and M. Ernzerhof, Generalized Gradient Approximation Made Simple, *Phys. Rev. Lett.*, 1996, **77**, 3865–3868.

5 S. Grimme, J. Antony, S. Ehrlich and H. Krieg, A consistent and accurate ab initio parametrization of density functional dispersion correction (DFT-D) for the 94 elements H-Pu, *J. Chem. Phys.*, , DOI:10.1063/1.3382344.

6 E. Sanville, S. D. Kenny, R. Smith and G. Henkelman, Improved grid-based algorithm for Bader charge allocation, *J. Comput. Chem.*, 2007, **28**, 899–908.